

A Revised Shear-Lag Analysis of an Energy Model for Fiber-Matrix Debonding

John A. Nairn* and H. Daniel Wagner†

*Material Science & Engineering, University of Utah, Salt Lake City, Utah 84112, USA

†Department of Materials and Interfaces, Weizmann Institute of Science, Rehovot 76100, Israel

A shear-lag analysis based on energy is used to predict the amount of debonding that occurs when a fiber fragment breaks into two fragments. The shear-lag analysis reproduces all features of more sophisticated analyses. A drawback of the shear-lag analysis, however, is that it depends on an unknown parameter which can be expressed in terms of an *effective* fiber volume fraction. If the *effective* fiber volume fraction can be determined (by experiments or by advanced stress analyses), the shear-lag model can be used to interpret debonding experiments.

Introduction

Reference [1] proposed that the extent of debonding during a single fiber fragmentation test can be predicted by equating the total energy released due to fiber fracture to the energy required to create fiber fracture and debond fracture surface area. Using this hypothesis and a one dimensional shear-lag analysis, an expression was derived that predicts the initial debond length as a function of applied stress level. This analysis was limited to long fragments, ignored residual thermal stresses, and assumed frictionless debonds.

There have been two developments since Ref. [1]. First, some general tools for energy analysis of fragmentation specimens have been derived [2]. By using the results in Ref. [2], we can extend the previous shear-lag debonding analysis to work for all fragment lengths, and to include residual stresses. Second, both the limitations and capabilities of shear-lag analysis for fiber-matrix stress transfer have been assessed [3]. By using the results in Ref. [3], we can recommend some minor revisions to the shear-lag analysis in Ref. [1]. Furthermore, we can examine the limitations and capabilities of shear-lag debonding analyses.

Revised Theory

In a fragmentation test, a single fiber is embedded in a large amount of matrix and the specimen is loaded until the fiber breaks into fragments. In Ref. [2], the total strain energy in a single fragment within a fragmentation specimen with an intact and perfect interface was derived to be

$$U(\rho) = \rho U_0 + \pi r_f^2 \sigma_{f\infty}^2 \langle w_f^{(p)}(\rho) \rangle \quad (1)$$

where $\rho = l/(2r_f)$ is the aspect ratio of the fiber fragment (of length l and radius r_f), $\sigma_{f\infty}$ is the far-field fiber stress (the fiber stress far-away from a fiber break in an infinitely long fragment), and ρU_0 is the far-field strain energy. In terms of fiber and matrix properties, applied stress (σ_0), and temperature differential (ΔT), the far-field fiber stress is [2]:

$$\sigma_{f\infty} = \frac{\left(\frac{2\nu_A\nu_m}{E_A} - \frac{1-\nu_T}{E_T} - \frac{1+\nu_m}{E_m} \right) \frac{E_A\sigma_0}{E_m} + \left(\frac{2\nu_A}{E_A}(\alpha_T - \alpha_m) + \left(\frac{1-\nu_T}{E_T} + \frac{1+\nu_m}{E_m} \right) (\alpha_A - \alpha_m) \right) E_A\Delta T}{\frac{2\nu_A^2}{E_A} - \frac{1-\nu_T}{E_T} - \frac{1+\nu_m}{E_m}} \quad (2)$$

The anisotropic fiber is assumed to be transversely isotropic. The terms E_A , E_T , ν_A , ν_T , α_A , and α_T are the axial (fiber direction) and transverse moduli, Poisson's ratios, and thermal expansion coefficients of the fiber. The terms E_m , ν_m , and α_m are the modulus, Poisson's ratio, and thermal expansion coefficient of the isotropic matrix.

The term $\langle w_f^{(p)}(\rho) \rangle$ in Eq. (1) is the average fiber displacement on the end of the fiber. The superscript (p) denotes a “perturbation” fiber displacement or the fiber displacement due to compression stress of -1 on the fiber ends and zero displacement on the matrix ends [2]. Equation (1) is exact provided we supply an exact result for $\langle w_f^{(p)}(\rho) \rangle$. Here we will use shear-lag methods to derive an approximate $\langle w_f^{(p)}(\rho) \rangle$ and therefore an approximate strain energy. The shear-lag equation for average axial fiber stress is

$$\frac{\partial^2 \langle \sigma_f \rangle}{\partial \zeta^2} - \beta^2 \langle \sigma_f \rangle = -\beta^2 \langle \sigma_{f\infty} \rangle \quad (3)$$

where β is a dimensionless shear-lag parameter and ζ is a dimensionless axial coordinate ($\zeta = z/r_f$). This equation was first used by Cox [4] who further claimed the shear-lag parameter to be

$$\beta_{\text{cox}}^2 = -\frac{4\mu_m}{E_f \ln V_f} \quad (4)$$

where μ_m is the shear modulus of the matrix and V_f is the volume fraction of the fiber. A careful examination of shear-lag analysis, however, shows β_{cox} to be an extremely poor choice for modeling fiber/matrix stress transfer [3]. An alternate parameter first derived by Nayfeh [5] works much better:

$$\beta^2 = \frac{2}{E_A E_m} \left[\frac{E_A V_f + E_m V_m}{\frac{V_m}{4\mu_A} + \frac{1}{2\mu_m} \left(\frac{1}{V_m} \ln \frac{1}{V_f} - 1 - \frac{V_m}{2} \right)} \right] \quad (5)$$

where μ_A is the axial shear modulus of the fiber and V_m is the volume fraction of the matrix. β_{cox} was used in the previous debonding analysis [1]. An important revision made here is to replace β_{cox} by β in Eq. (5).

We consider a fiber fragment with the origin at the center of the fragment. The boundary conditions for the perturbation stresses are $\langle \sigma_f(\pm\rho) \rangle = -1$. The shear-lag solution is easily found to be

$$\langle \sigma_f \rangle = -\frac{\cosh \beta \zeta}{\cosh \beta \rho} \quad \text{and} \quad \langle w_f^{(p)}(\rho) \rangle = \frac{r_f}{E_A} \int_0^\rho \langle \sigma_f \rangle d\zeta = -\frac{r_f \tanh \beta \rho}{E_A \beta} \quad (6)$$

An approximate expression for strain energy in a fiber fragment becomes

$$U(\rho) = \rho U_0 - \pi r_f^3 \sigma_{f\infty}^2 F(\rho) \quad \text{where} \quad F(\rho) = \frac{\tanh \beta \rho}{E_A \beta} \quad (7)$$

The analysis in Ref. [2] developed results for fiber fracture and debonding based solely on the fragment energy and expressed in terms of an analogous energy function $F(\rho)$. In Ref. [2], $F(\rho)$ was found by a complicated, axisymmetric analysis of the fragmentation specimen stresses; here we generate simpler shear-lag results simply by using the results from Ref. [2] but substituting instead $F(\rho)$ from Eq. (7). When the two fragment ends each have debonds of length $L_d/2$, the total fragment strain energy changes to [2]:

$$U(\rho, \delta) = \rho U_0 - \pi r_f^3 \sigma_{f\infty}^2 \left[\frac{\delta Q}{E_A} + F(\rho - \delta) \right] \quad (8)$$

where $\delta = L_d/2r_f$ is the dimensionless length of *each* debond and

$$Q = 1 - \frac{\frac{2\nu_A^2}{E_A}}{\frac{1+\nu_m}{E_m} + \frac{1-\nu_T}{E_T}} \quad (9)$$

Q is approximately 1 when $E_A \gg E_m$; it accounts for strain energy associated with radial and hoop stresses within the debond zone [2]. The energy release rates for fiber fracture, G_f , and for debonding, G_d , are [2]:

$$G_f(\rho, \delta) = r_f \sigma_{f\infty}^2 \left[2F\left(\frac{\rho - \delta}{2}\right) - F(\rho - \delta) \right] = \frac{r_f \sigma_{f\infty}^2}{E_A \beta} \left(2 \tanh \frac{\beta(\rho - \delta)}{2} - \tanh \beta(\rho - \delta) \right) \quad (10)$$

$$G_d(\rho, \delta) = \frac{r_f \sigma_{f\infty}^2}{4} \left[\frac{Q}{E_A} - F'(\rho - \delta) \right] = \frac{r_f \sigma_{f\infty}^2}{4E_A} \left[Q - \operatorname{sech}^2 \beta(\rho - \delta) \right] \quad (11)$$

The debonding energy release rate reduces to the Outwater and Murphy [6] result in the limit of $(\rho - \delta) \rightarrow \infty$ provided Q is taken as equal to 1 (because they ignored radial and hoop stresses in the debond zone).

Using an energy analysis [1, 2], we *assume* that when a fragment of aspect ratio ρ having two initial debonds of length δ_i breaks into two fragments of aspect ratio $\rho/2$ each with two debonds of length δ_f , that the total amount of new debonding, $\delta^* = 4\delta_f - 2\delta_i$, can be predicted by equating the total energy released by fiber fracture and debonding to the total energy required to create the new fiber fracture and debond fracture surfaces. Note, the analysis is unaffected by unequal debond lengths on the two fiber ends; δ_i and δ_f can thus be taken as *average* debond lengths before and after the fiber break. The energy balance expression is [1, 2]:

$$\pi r_f^2 G_f(\rho - \delta_i, 0) + 8\pi r_f^2 \int_{\delta_i/2}^{\delta_f} G_d\left(\frac{\rho}{2}, \delta\right) d\delta = \pi r_f^2 \Gamma_f + 2\pi r_f^2 \Gamma_d \delta^* \quad (12)$$

where Γ_f and Γ_d are the average fiber and interface toughnesses. The result after partially solving for δ^* is

$$\delta^* = \frac{\frac{2r_f \sigma_{f\infty}^2}{\beta} \left[2 \tanh\left(\frac{\beta(\rho - \delta_i)}{2}\right) - \frac{\beta \delta^*}{4} \right] - 2E_A \Gamma_f}{4E_A \Gamma_d - r_f \sigma_{f\infty}^2 Q} \quad (13)$$

When coupled with actual or predicted fragmentation data (*i.e.*, fragment aspect ratio as a function of applied stress), Eq. (13) can predict the amount of debonding associated with each fiber break. Alternatively, when coupled with debond observations, Eq. (13) can be used to determine interfacial debonding energy (Γ_d). Thus, Eq. (13) is the revised shear-lag debonding model that extends the model in Ref. [1] to work for all fragment lengths, to include residual thermal stresses (through terms in $\sigma_{f\infty}$), and to use improved shear-lag analysis (through the improved β in Eq. (5)). The shear-lag debonding model is based only on shear-lag calculations of average fiber stress and total strain energy. As discussed in Ref. [3], shear-lag is qualitatively accurate for these quantities; thus this shear-lag debonding model should give reasonable results. In contrast, shear-lag debonding models that are based on interfacial shear stresses should not be used because shear-lag analysis gives unreliable results for shear stresses [3].

Equation (13) must be solved numerically because δ^* appears as an argument in $\tanh(x)$. The situation simplifies in the long-fragment limit where $\lim_{x \rightarrow \infty} \tanh(x) \rightarrow 1$ and an analytical expression for δ^* is

$$\delta^* = \frac{L_d}{r_f} = \frac{\frac{2r_f \sigma_{f\infty}^2}{\beta} - 2E_A \Gamma_f}{4E_A \Gamma_d - r_f \sigma_{f\infty}^2 Q} \quad (14)$$

The analogous result in Ref. [1] was

$$\frac{L_d}{r_f} \text{ (old model)} = \frac{2r_f \sigma_f^2 \left(\frac{1}{\beta_{\text{cox}}} - \frac{\beta_{\text{cox}} E_A}{16\mu_A} \right) - 2E_A \Gamma_f}{4E_A \Gamma_d - r_f \sigma_f^2} \quad (15)$$

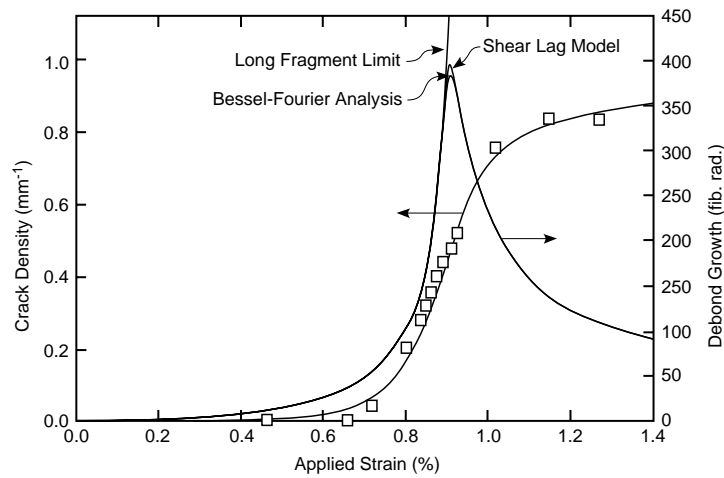


Figure 1. Debonding predictions by shear-lag model, Bessel-Fourier model, and long-fragment limit model during fragmentation of a carbon fiber ($E_A=390$ GPa, $E_T=14$ GPa, $\mu_A=20$ GPa, $\nu_A=0.2$, $\nu_T=0.25$, $r_f=3.5$ μm) in an epoxy matrix ($E_m=2.6$ GPa, $\nu_m=0.34$) (data from Ref. [7]).

The forms of the new model (Eq. (14)) and of the old model (Eq. (15)) are the same. The new model, however, includes residual thermal stresses (through $\sigma_{f\infty}$ instead of σ_f), uses the improved shear lag parameter (β instead of β_{cox}), and includes the factor Q . The previous model had an additional term in the numerator that is proportional to E_A/μ_A . That term occurs because in Ref. [1], strain energy was calculated by integrating strain energy density; the extra term arose from the shear stress terms in the strain energy density. Although mathematically correct, it is unlikely that the integral approach is more accurate than the strain energy analysis based on perturbation fiber displacement (see Eq. (1) [2, 3]).

Results and Discussion

In Ref. [2] a set of fragmentation data for a high-modulus carbon fiber in an epoxy matrix [7] was modeled by assuming that the fiber fragments when the peak stress in the fiber reaches the length-dependent strength of the fiber and that each fiber break is associated with debond growth. The fiber strength was experimentally determined to be $\sigma_{ult}(l) = 3750 - 817 \log l$ (in MPa when l in mm) [7]. The debond growth, although not measured, was predicted using the energy balance method [1, 2] with $\Gamma_d = 30.5$ J/m² and $\Gamma_f = 10$ J/m². The debonding toughness was determined by fitting the predictions to the fragmentation data; the fiber toughness was selected arbitrarily but has little influence on the predictions as long as it is much less than the amount of energy released by fiber breaks (about 4000 J/m² [2]). In Ref. [2] the debond predictions were made using an axisymmetric stress analysis based on a Bessel-Fourier series stress function. Here we compare the full Bessel-Fourier analysis results to the much simpler shear-lag model.

Figure 1 shows typical fragmentation data and energy model predictions of the amount of debonding associated with each fiber break. The shear-lag model and Bessel-Fourier model are virtually identical. They both rise to a peak and then decrease as the fragmentation process approaches saturation. The shear lag model has a slightly higher peak than the Bessel-Fourier analysis. Also shown in Fig. 1 is the debond growth predicted by the long-fragment limit result (see Eq. (14)). The long fragment limit is accurate prior to the peak in the full analysis results. The shear-lag and Bessel-Fourier analysis results are identical in the long fragment limit.

The shear-lag predictions in Fig. 1 depend on the value of β , but, it is formally not possible to determine β for a single fiber in a large amount of matrix. The problem is that as $V_f \rightarrow 0$, β incorrectly approaches zero. In other words, shear-lag analysis does not correctly model

stress transfer at very low V_f [3]. The only recourse, is to treat β as an unknown parameter; the traditional approach is to define an *effective* V_f . Looking at fiber stress (see Eq. (6)), an *effective* β can be estimated from the number of fiber diameters required to transfer 50% of the far-field fiber stress back into the fiber:

$$\zeta_{50} = \frac{1}{\beta} \cosh^{-1} \left(\frac{1}{2} \cosh \beta \rho \right) \quad (16)$$

Alternatively, from Eq. (10), β can be found from the long fragment limit for fiber energy release rate

$$\beta = \frac{r_f \sigma_{f\infty}^2}{E_A} \frac{1}{\lim_{\rho \rightarrow \infty} G_f(\rho)} \quad (17)$$

The later approach was used here with $G_f(\rho)$ given by the Bessel-Fourier analysis in Ref. [2]. For the carbon fiber/epoxy system, the effective V_f was 0.16%. For other systems, the *effective* V_f depends on the fiber and matrix mechanical properties and on the ability of the fiber/matrix interface to transfer stress. The effective V_f increases as the modulus ratio E_A/E_m decreases and decreases as the stress transfer efficiency gets worse [2]. In summary, the shear-lag debonding model reproduces all features of more complicated models, but it depends on an unknown parameter — the *effective* V_f . Before shear-lag analysis can be used to interpret experiments, the *effective* V_f must be determined by comparison to stress transfer experiments or by calibration using more advanced analyses that do not have unknown parameters (*e.g.*, the Bessel-Fourier analysis in Ref. [2]).

It is possible that not all the energy released by fiber breaks will be consumed by debonding. For example some energy could be dissipated as heat, vibrations, or friction on the debond surface. To a first approximation, effects of other energy dissipation mechanisms can be included by reducing the value of Q . This change will not change the form of any of the debond predictions or of fits to experimental data, but it will change the value of Γ_d required to generate the fits. Specially, the Γ_d determined from a frictionless model is an upper bound to the true debonding toughness.

Acknowledgements

This work was supported, in part, by a grant from the Mechanics of Materials program at NSF (CMS-9401772), and, in part, by a grant from the United States-Israel Binational Science Foundation (BSF Grant No. 92-00170), Jerusalem, Israel.

References

1. H. D. Wagner, J. A. Nairn, and M. Detassis, "Toughness of Interfaces from Initial Fiber-Matrix Debonding in a Single-Fiber Composite Fragmentation Test," *Applied Comp. Mater.*, **2** (1995) 107–117.
2. J. A. Nairn and Y. C. Liu, "On the Use of Energy Methods for Interpretation of Results of Single-Fiber Fragmentation Experiments," *Composite Interfaces*, in press (1996).
3. J. A. Nairn, "On the Use of Shear-Lag Methods for Analysis of Stress Transfer in Unidirectional Composites," *Mech. of Materials*, submitted (1996).
4. H. L. Cox, "The Elasticity and Strength of Paper and Other Fibrous Materials," *Brit. J. Appl. Phys.*, **3** (1952) 72–79.
5. A. H. Nayfeh, "Thermomechanically Induced Interfacial Stresses in Fibrous Composites," *Fibre Sci. & Tech.*, **10** (1977) 195–209.
6. J. O. Outwater and M. C. Murphy, "Fracture Energy of Unidirectional Laminates," *Modern Plastics*, **47 (Sept.)** (1970) 160–169.
7. Y. Huang and Young R. J., "Analysis of the Fragmentation Test for Carbon Fibre/Epoxy Model Composites Using Raman Spectroscopy," *Comp. Sci. & Tech.*, **52** (1994) 505–517.